



Results on Neutrinoless Double- β Decay of ^{76}Ge from Phase I of the GERDA Experiment

M. Agostini,¹⁴ M. Allardt,³ E. Andreotti,^{17,5} A. M. Bakalyarov,¹² M. Balata,¹ I. Barabanov,¹⁰ M. Barnabé Heider,^{6,14,*} N. Barros,³ L. Baudis,¹⁸ C. Bauer,⁶ N. Becerici-Schmidt,¹³ E. Bellotti,^{7,8} S. Belogurov,^{11,10} S. T. Belyaev,¹² G. Benato,¹⁸ A. Bettini,^{15,16} L. Bezrukov,¹⁰ T. Bode,¹⁴ V. Brudanin,⁴ R. Brugnera,^{15,16} D. Budjáš,¹⁴ A. Caldwell,¹³ C. Cattadori,⁸ A. Chernogorov,¹¹ F. Cossavella,¹³ E. V. Demidova,¹¹ A. Domula,³ V. Egorov,⁴ R. Falkenstein,¹⁷ A. Ferella,^{18,†} K. Freund,¹⁷ N. Frodyma,² A. Gangapshev,^{10,6} A. Garfagnini,^{15,16} C. Gotti,^{8,‡} P. Grabmayr,¹⁷ V. Gurentsov,¹⁰ K. Gusev,^{12,4,14} K. K. Guthikonda,¹⁸ W. Hampel,⁶ A. Hegai,¹⁷ M. Heisel,⁶ S. Hemmer,^{15,16} G. Heusser,⁶ W. Hofmann,⁶ M. Hult,⁵ L. V. Inzhechik,^{10,§} L. Ioannucci,¹ J. Janicskó Csáthy,¹⁴ J. Jochum,¹⁷ M. Junker,¹ T. Kihm,⁶ I. V. Kirpichnikov,¹¹ A. Kirsch,⁶ A. Klimenko,^{4,6,||} K. T. Knöpfle,⁶ O. Kochetov,⁴ V. N. Kornoukhov,^{11,10} V. V. Kuzminov,¹⁰ M. Laubenstein,¹ A. Lazzaro,¹⁴ V. I. Lebedev,¹² B. Lehnert,³ H. Y. Liao,¹³ M. Lindner,⁶ I. Lippi,¹⁶ X. Liu,^{13,¶} A. Lubashevskiy,⁶ B. Lubsandorzhev,¹⁰ G. Lutter,⁵ C. Macolino,¹ A. A. Machado,⁶ B. Majorovits,¹³ W. Maneschg,⁶ M. Misiaszek,² I. Nemchenok,⁴ S. Nisi,¹ C. O'Shaughnessy,^{13,**} L. Pandola,¹ K. Pelczar,² G. Pessina,^{8,7} A. Pullia,⁹ S. Riboldi,⁹ N. Rumyantseva,⁴ C. Sada,^{15,16} M. Salathe,⁶ C. Schmitt,¹⁷ J. Schreiner,⁶ O. Schulz,¹³ B. Schwingenheuer,⁶ S. Schönert,¹⁴ E. Shevchik,⁴ M. Shirchenko,^{12,4} H. Simgen,⁶ A. Smolnikov,⁶ L. Stanco,¹⁶ H. Strecker,⁶ M. Tarka,¹⁸ C. A. Ur,¹⁶ A. A. Vasenko,¹¹ O. Volynets,¹³ K. von Sturm,^{15,16} V. Wagner,⁶ M. Walter,¹⁸ A. Wegmann,⁶ T. Wester,³ M. Wojcik,² E. Yanovich,¹⁰ P. Zavarise,^{1,††} I. Zhitnikov,⁴ S. V. Zhukov,¹² D. Zinatulina,⁴ K. Zuber,³ and G. Zuzel²

(GERDA Collaboration)^{‡‡}

¹*INFN Laboratori Nazionali del Gran Sasso, LNGS, Assergi, Italy*

²*Institute of Physics, Jagiellonian University, Cracow, Poland*

³*Institut für Kern- und Teilchenphysik, Technische Universität Dresden, Dresden, Germany*

⁴*Joint Institute for Nuclear Research, Dubna, Russia*

⁵*Institute for Reference Materials and Measurements, Geel, Belgium*

⁶*Max-Planck-Institut für Kernphysik, Heidelberg, Germany*

⁷*Dipartimento di Fisica, Università Milano Bicocca, Milano, Italy*

⁸*INFN Milano Bicocca, Milano, Italy*

⁹*Dipartimento di Fisica, Università degli Studi di Milano e INFN Milano, Milano, Italy*

¹⁰*Institute for Nuclear Research of the Russian Academy of Sciences, Moscow, Russia*

¹¹*Institute for Theoretical and Experimental Physics, Moscow, Russia*

¹²*National Research Centre "Kurchatov Institute", Moscow, Russia*

¹³*Max-Planck-Institut für Physik, München, Germany*

¹⁴*Physik Department and Excellence Cluster Universe, Technische Universität München, Germany*

¹⁵*Dipartimento di Fisica e Astronomia dell'Università di Padova, Padova, Italy*

¹⁶*INFN Padova, Padova, Italy*

¹⁷*Physikalisches Institut, Eberhard Karls Universität Tübingen, Tübingen, Germany*

¹⁸*Physik Institut der Universität Zürich, Zürich, Switzerland*

(Received 17 July 2013; published 19 September 2013)

Neutrinoless double beta decay is a process that violates lepton number conservation. It is predicted to occur in extensions of the standard model of particle physics. This Letter reports the results from phase I of the Germanium Detector Array (GERDA) experiment at the Gran Sasso Laboratory (Italy) searching for neutrinoless double beta decay of the isotope ^{76}Ge . Data considered in the present analysis have been collected between November 2011 and May 2013 with a total exposure of 21.6 kg yr. A blind analysis is performed. The background index is about 1×10^{-2} counts/(keV kg yr) after pulse shape discrimination. No signal is observed and a lower limit is derived for the half-life of neutrinoless double beta decay of ^{76}Ge , $T_{1/2}^{0\nu} > 2.1 \times 10^{25}$ yr (90% C.L.). The combination with the results from the previous experiments with ^{76}Ge yields $T_{1/2}^{0\nu} > 3.0 \times 10^{25}$ yr (90% C.L.).

DOI: [10.1103/PhysRevLett.111.122503](https://doi.org/10.1103/PhysRevLett.111.122503)

PACS numbers: 23.40.-s, 21.10.Tg, 27.50.+e, 29.40.Wk

Introduction.—For several isotopes beta decay is energetically forbidden but the simultaneous occurrence of two beta decays ($2\nu\beta\beta$) is allowed. This process has been observed in 11 nuclei with half-lives in the range of 10^{18} – 10^{24} yr [1,2]. Extensions of the standard model predict that also neutrinoless double beta ($0\nu\beta\beta$) decay should exist: $(A, Z) \rightarrow (A, Z + 2) + 2e^-$. In this process lepton number is violated by two units and the observation would have far-reaching consequences [3–6]. It would prove that neutrinos have a Majorana mass component. Assuming the exchange of light Majorana neutrinos, an effective neutrino mass can be evaluated by using predictions for the nuclear matrix element (NME).

The experimental signature of $0\nu\beta\beta$ decay is a peak at the Q value of the decay. The two most sensitive experiments with the candidate nucleus ^{76}Ge ($Q_{\beta\beta} = 2039.061 \pm 0.007$ keV [7]) were Heidelberg-Moscow (HDM) [8] and the International Germanium Experiment (IGEX) [9,10]. They found no evidence for the $0\nu\beta\beta$ decay of ^{76}Ge and set lower limits on the half-life $T_{1/2}^{0\nu} > 1.9 \times 10^{25}$ yr and $> 1.6 \times 10^{25}$ yr at 90% C.L., respectively. Part of the HDM group published a claim to have observed (28.75 ± 6.86) $0\nu\beta\beta$ decays [11] and reported $T_{1/2}^{0\nu} = (1.19^{+0.37}_{-0.23}) \times 10^{25}$ yr. Later, pulse shape information was used to strengthen the claim [12]. Because of inconsistencies in the latter pointed out recently [13], the present comparison is restricted to the result of Ref. [11].

Until recently, the claim has not been scrutinized. The currently most sensitive experiments are KamLAND-Zen [14] and EXO-200 [15] looking for $0\nu\beta\beta$ decay of ^{136}Xe and GERDA [16] employing ^{76}Ge . NME calculations are needed to relate the different isotopes. Thus the experiments using ^{136}Xe cannot refute the claim in a model-independent way. GERDA is able to perform a direct test using the same isotope and also using mostly the same detectors as HDM and IGEX. This Letter reports the $0\nu\beta\beta$ results of phase I of GERDA.

The experiment.—The GERDA experiment [16] is located at the Laboratori Nazionali del Gran Sasso (LNGS) of INFN in Italy. High-purity germanium (HPGe) detectors made from isotopically modified material with ^{76}Ge enriched to $\sim 86\%$ ($^{\text{enr}}\text{Ge}$) are mounted in low-mass copper supports and immersed in a 64 m^3 cryostat filled with liquid argon (LAr). The LAr serves as the cooling medium and shield against external backgrounds. The shielding is complemented by 3 m of water, which is instrumented with photomultipliers to detect Cherenkov light generated by muons. The HPGe detector signals are read out with custom-made charge sensitive amplifiers optimized for low radioactivity which are operated close to the detectors in the LAr. The analog signals are digitized with 100 MHz flash analog-to-digital converters (ADCs) and analyzed off-line. If one of the detectors has an energy deposition above the trigger threshold (40–100 keV), all channels are analyzed for possible coincidences.

Reprocessed p -type semicoaxial detectors from the HDM and IGEX experiments were operated together with newly produced GERDA phase II detectors. The latter are of broad energy germanium (BEGe) type manufactured by Canberra [17]. The active volume fraction f_{av} of the detectors was determined beforehand amounting to 0.87 (0.92) for the semicoaxial (BEGe) detectors [16,18].

Data acquisition started in November 2011 with eight $^{\text{enr}}\text{Ge}$ detectors (ANG 1–5 from HDM and RG 1–3 from IGEX), totaling a weight of 17.67 kg. Five enriched GERDA phase II detectors of 3.63 kg in total were deployed in July 2012. ANG 1 and RG 3 started to draw leakage current soon after their deployment, and are omitted in this analysis. One BEGe detector showed an unstable behavior and is omitted as well. Since March 2013, RG 2 has no longer been used since it is operated below its full depletion voltage. A fraction of 5% of the data was discarded because of temperature-related instabilities. Results from the data collected until May 2013 (492.3 live days) are reported here. The total exposure considered for the analysis amounts to 21.6 kg yr of $^{\text{enr}}\text{Ge}$ detector mass, yielding (215.2 ± 7.6) mol yr of ^{76}Ge within the active volume.

The offline analysis of the digitized charge pulses is performed with the software tool GELATIO [19] and the procedure described in Ref. [20]. The deposited energy is reconstructed by a digital filter with semi-Gaussian shaping. Events generated by discharges or due to electromagnetic noise are rejected by a set of quality cuts.

The energy scale of the individual detectors is determined with ^{228}Th sources once every one or two weeks. The differences between the reconstructed peak positions and the ones from the calibration curves are smaller than 0.3 keV. The energy resolution was stable over the entire data acquisition period. The gain variation between consecutive calibrations is less than 0.05% [16], which corresponds to $< 30\%$ of the expected energy resolution [full width at half maximum (FWHM)] at $Q_{\beta\beta}$. Between calibrations, the stability is monitored by regularly injecting charge pulses into the input of the amplifiers.

The energy spectrum and its decomposition into individual sources is discussed in Ref. [18]. Peaks from ^{40}K , ^{42}K , ^{214}Bi , ^{214}Pb , and ^{208}Tl γ rays can be identified as well as α decays from the ^{226}Ra decay chain, and β events from ^{39}Ar . All γ -ray peaks are reconstructed at the correct energy within their statistical uncertainty. The energy resolution (FWHM) of the strongest line (1524.6 keV from ^{42}K) is 4.5 (3.1) keV for the semicoaxial (BEGe) detectors. These values are about 10% larger than the resolutions obtained from calibrations. The broadening is due to fluctuations of the energy scale between calibrations. The interpolated FWHM at $Q_{\beta\beta}$ for physics data is detector dependent and varies between 4.2 and 5.7 keV for the semicoaxial detectors, and between 2.6 and 4.0 keV for the BEGe detectors. The exposure-averaged values are (4.8 ± 0.2) keV and (3.2 ± 0.2) keV, respectively.

The corresponding standard deviations σ_E are used for fitting a possible peak at $Q_{\beta\beta}$.

A blind analysis was performed in order to avoid bias in the event selection criteria, which has not been done before in the field of the search for $0\nu\beta\beta$ decay. Events with energies within $Q_{\beta\beta} \pm 20$ keV were not processed. After the energy calibration and the background model were finalized the window was opened except for ± 5 keV (± 4 keV) around $Q_{\beta\beta}$ for the semicoaxial (BEGe) detectors. After all selections discussed below had been frozen, the data in the $Q_{\beta\beta}$ region were analyzed. The validity of the off-line energy reconstruction and of the event selection procedures have been cross-checked with a fully independent analysis.

$0\nu\beta\beta$ analysis.—The signature for $0\nu\beta\beta$ decay is a single peak at $Q_{\beta\beta}$. Furthermore, events from $0\nu\beta\beta$ decays have a distinct topology, which allows us to distinguish them from γ -induced background. For $0\nu\beta\beta$ events, energy is deposited by the two electrons, which have a short range in germanium: more than 90% of $0\nu\beta\beta$ events are expected to deposit all energy localized within a few mm³ [single-site events (SSE)]. On the other hand, most background events from γ -ray interactions have energy depositions in many detectors or at different, well separated, positions [multisite events (MSE)].

Only events with an energy deposition in a single detector are accepted resulting in a background reduction by about 15% around $Q_{\beta\beta}$, with no efficiency loss for $0\nu\beta\beta$ decays. Events in the HPGe detectors are rejected if they are in coincidence within 8 μ s with a signal from the muon veto. This leads to a further background reduction by about 7%. Events that are preceded or followed by another event in the same detector within 1 ms are excluded. This allows us to reject background events from the ^{214}Bi - ^{214}Po cascade (BiPo) in the ^{222}Rn decay chain. Less than 1% of the events at $Q_{\beta\beta}$ are affected by this cut. Due to the low counting rate in GERDA and due to the low muon flux at LNGS, the dead time due to the muon veto and BiPo cuts is negligible.

The detector signals are different for SSE and MSE, and also surface events from β or α decays exhibit a characteristic shape. Thus, pulse shape discrimination (PSD) techniques can improve the sensitivity.

For BEGe detectors, a simple and effective PSD is based on the ratio of the maximum of the current pulse (called A) over the energy E [21–23]. The A/E cut efficiency is determined from calibration data using events in the double escape peak (DEP) of the 2615 keV γ ray from ^{208}Tl . It is cross-checked with $2\nu\beta\beta$ decays of ^{76}Ge . The acceptance of signal events at $Q_{\beta\beta}$ is $\epsilon_{\text{PSD}} = 0.92 \pm 0.02$, while only 20% of the background events at this energy survive.

For the semicoaxial detectors, a PSD method based on an artificial neural network (ANN) [23] is used. The signal acceptance $\epsilon_{\text{psd}} = 0.90_{-0.09}^{+0.05}$ is adjusted with DEP events and the uncertainty is derived from the $2\nu\beta\beta$ spectrum and

from events at the Compton edge. About 55% of the background events around $Q_{\beta\beta}$ are classified as SSE-like and considered for the analysis. Two alternative PSD methods were developed based on a likelihood ratio and on a combination of A/E and the asymmetry of the current pulse; they are used for cross-checks. The three PSD methods use very different training samples and selection criteria but more than 90% of the events rejected by ANN are also rejected by the two other algorithms.

The half-life on $0\nu\beta\beta$ decay is calculated as

$$T_{1/2}^{0\nu} = \frac{(\ln 2) N_A}{m_{\text{enr}} N^{0\nu}} \mathcal{E} \epsilon, \quad (1)$$

$$\epsilon = f_{76} f_{\text{av}} \epsilon_{\text{FEP}} \epsilon_{\text{PSD}}, \quad (2)$$

with N_A being Avogadro's constant, \mathcal{E} the total exposure (detector mass \times live time), and $m_{\text{enr}} = 75.6$ g the molar mass of the enriched material. $N^{0\nu}$ is the observed signal strength or the corresponding upper limit. The efficiency ϵ accounts for the fraction of ^{76}Ge atoms (f_{76}), the active volume fraction (f_{av}), the signal acceptance by PSD (ϵ_{PSD}), and the efficiency for detecting the full energy peak ϵ_{FEP} . The latter is the probability that a $0\nu\beta\beta$ decay taking place in the active volume of a detector releases its entire energy in it, contributing to the full energy peak at $Q_{\beta\beta}$. Energy losses are due to bremsstrahlung photons, fluorescence x rays, or electrons escaping the detector active volume. Monte Carlo simulations yield $\epsilon_{\text{FEP}} = 0.92$ (0.90) for semicoaxial (BEGe) detectors.

The GERDA background model [18] predicts approximately a flat energy distribution between 1930 and 2190 keV from Compton events of γ rays of ^{208}Tl and ^{214}Bi decays, degraded α events, and β rays from ^{42}K and ^{214}Bi . The signal region (2039 ± 5) keV and the intervals (2104 ± 5) keV and (2119 ± 5) keV, which contain known γ -ray peaks from ^{208}Tl and ^{214}Bi , respectively, are excluded in the background calculation. The net width of the window used for the evaluation of the constant background is hence 230 keV.

Data are grouped into three subsets with similar characteristics: (i) data from the BEGe detectors form one set, (ii) the golden data set contains the major part of the data from the semicoaxial detectors except (iii) two short periods with higher background levels when the BEGe detectors were inserted (silver data set).

Results.—Table I lists the observed number of events in the interval $Q_{\beta\beta} \pm 5$ keV for the three data sets, the number of background events in the 230 keV window, and the exposure-weighted average efficiency (ϵ) over all detectors. Table II reports the details of these events including the results from the PSD analysis. The combined energy spectrum around $Q_{\beta\beta}$, with and without the PSD selection, is displayed in Fig. 1.

Seven events are observed in the range $Q_{\beta\beta} \pm 5$ keV before the PSD, to be compared to 5.1 ± 0.5 expected

TABLE I. Parameters for the three data sets with and without the pulse shape discrimination (PSD). “Background” (bkg) is the number of events in the 230 keV window and BI is the respective background index, calculated as $\text{bkg}/(\mathcal{E} \times 230 \text{ keV})$. “Counts” refers to the observed number of events in the interval $Q_{\beta\beta} \pm 5 \text{ keV}$.

Data set	\mathcal{E} (kg yr)	$\langle \epsilon \rangle$	Background	BI ^a	Counts
Without PSD					
Golden	17.9	0.688 ± 0.031	76	18 ± 2	5
Silver	1.3	0.688 ± 0.031	19	63^{+16}_{-14}	1
BEGe	2.4	0.720 ± 0.018	23	42^{+10}_{-8}	1
With PSD					
Golden	17.9	$0.619^{+0.044}_{-0.070}$	45	11 ± 2	2
Silver	1.3	$0.619^{+0.044}_{-0.070}$	9	30^{+11}_{-9}	1
BEGe	2.4	0.663 ± 0.022	3	5^{+4}_{-3}	0

^aIn units of 10^{-3} counts/(keV kg yr).

background counts. No excess of events beyond the expected background is observed in any of the three data sets. This interpretation is strengthened by the pulse shape analysis. Of the six events from the semicoaxial detectors, three are classified as SSE by ANN, consistent with the expectation. Five of the six events have the same classification by at least one other PSD method. The event in the BEGe data set is rejected by the A/E cut. No events remain within $Q_{\beta\beta} \pm \sigma_E$ after PSD. All results quoted in the following are obtained with PSD.

To derive the signal strength $N^{0\nu}$ and a frequentist coverage interval, a profile likelihood fit of the three data sets is performed. The fitted function consists of a constant term for the background and a Gaussian peak for the signal with mean at $Q_{\beta\beta}$ and standard deviation σ_E . The fit has four free parameters: the backgrounds of the three data sets and $1/T_{1/2}^{0\nu}$, which relates to the peak integral by Eq. (1). The likelihood ratio is only evaluated for the physically allowed region $T_{1/2}^{0\nu} > 0$. It was verified that the method has always sufficient coverage. The systematic uncertainties due to the detector parameters, selection efficiency, energy resolution, and energy scale are folded in with a Monte Carlo approach, which takes correlations into account. The best fit value is $N^{0\nu} = 0$, namely no excess of signal events above the background. The limit on the half-life is

TABLE II. List of all events within $Q_{\beta\beta} \pm 5 \text{ keV}$.

Data set	Detector	Energy (keV)	Date	PSD passed
Golden	ANG 5	2041.8	18 Nov 2011 22:52	no
Silver	ANG 5	2036.9	23 Jun 2012 23:02	yes
Golden	RG 2	2041.3	16 Dec 2012 00:09	yes
BEGe	GD32B	2036.6	28 Dec 2012 09:50	no
Golden	RG 1	2035.5	29 Jan 2013 03:35	yes
Golden	ANG 3	2037.4	02 Mar 2013 08:08	no
Golden	RG 1	2041.7	27 Apr 2013 22:21	no

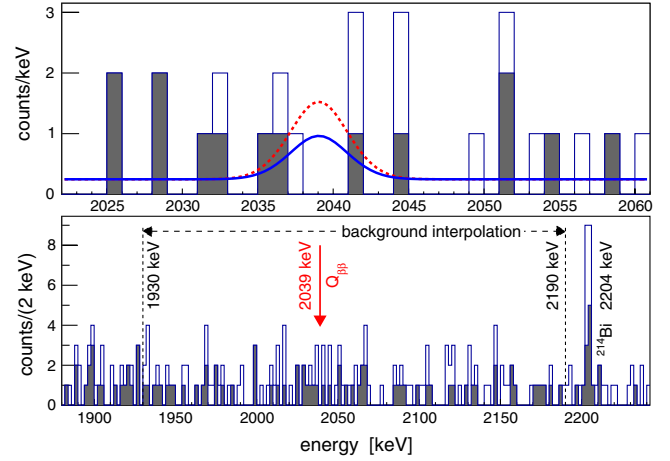


FIG. 1 (color online). The combined energy spectrum from all ^{76}Ge detectors without (with) PSD is shown by the open (filled) histogram. The lower panel shows the region used for the background interpolation. In the upper panel, the spectrum zoomed to $Q_{\beta\beta}$ is superimposed with the expectations (with PSD selection) based on the central value of Ref. [11] $T_{1/2}^{0\nu} = 1.19 \times 10^{25}$ yr (red dashed) and with the 90% upper limit derived in this work, corresponding to $T_{1/2}^{0\nu} = 2.1 \times 10^{25}$ yr (blue solid).

$$T_{1/2}^{0\nu} > 2.1 \times 10^{25} \text{ yr (90\% C.L.),} \quad (3)$$

including the systematic uncertainty. The limit on the half-life corresponds to $N^{0\nu} < 3.5$ counts. The systematic uncertainties weaken the limit by about 1.5%. Given the background levels and the efficiencies of Table I, the median sensitivity for the 90% C.L. limit is 2.4×10^{25} yr.

A Bayesian calculation [24] was also performed with the same fit described above. A flat prior distribution is taken for $1/T_{1/2}^{0\nu}$ between 0 and 10^{-24} yr^{-1} . The toolkit BAT [25] is used to perform the combined analysis on the data sets and to extract the posterior distribution for $T_{1/2}^{0\nu}$ after marginalization over all nuisance parameters. The best fit is again $N^{0\nu} = 0$ and the 90% credible interval is $T_{1/2}^{0\nu} > 1.9 \times 10^{25}$ yr (with folded systematic uncertainties). The corresponding median sensitivity is $T_{1/2}^{0\nu} > 2.0 \times 10^{25}$ yr.

Discussion.—The GERDA data show no indication of a peak at $Q_{\beta\beta}$, i.e., the claim for the observation of $0\nu\beta\beta$ decay in ^{76}Ge is not supported. Taking $T_{1/2}^{0\nu}$ from Ref. [11] at its face value, 5.9 ± 1.4 decays are expected (see the note in Ref. [26]) in $\Delta E = \pm 2\sigma_E$ and 2.0 ± 0.3 background events after the PSD cuts, as shown in Fig. 1. This can be compared with three events detected, none of them within $Q_{\beta\beta} \pm \sigma_E$. The model (H_1), which includes the $0\nu\beta\beta$ signal calculated above, gives in fact a worse fit to the data than the background-only model (H_0): the Bayes factor, namely the ratio of the probabilities of the two models, is $P(H_1)/P(H_0) = 0.024$. Assuming the model H_1 , the probability to obtain $N^{0\nu} = 0$ as the best fit from the profile likelihood analysis is $P(N^{0\nu} = 0|H_1) = 0.01$.

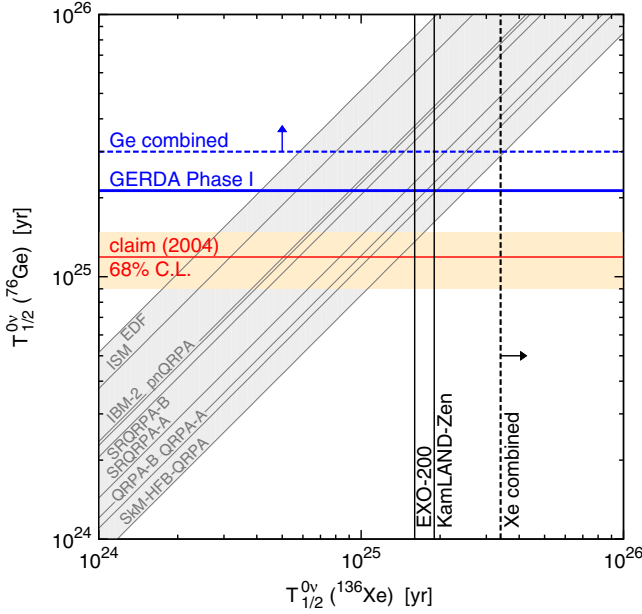


FIG. 2 (color online). Limits (90% C.L.) on $T_{1/2}^{0\nu}$ of ^{76}Ge (this work) and ^{136}Xe [14,15] compared with the signal claim for ^{76}Ge of Ref. [11] (68% C.L. band). The lines in the shaded gray band are the predictions for the correlation of the half-lives in ^{136}Xe and in ^{76}Ge according to different NME calculations [27,28,33–37]. The selection of calculations and the labels are taken from Ref. [29].

The GERDA result is consistent with the limits by HDM and IGEX. The profile likelihood fit is extended to include the energy spectra from HDM (interval 2000–2080 keV; Fig. 4 of Ref. [8]) and IGEX (interval 2020–2060 keV; Table II of Ref. [9]). Constant backgrounds for each of the five data sets and Gaussian peaks for the signal with common $1/T_{1/2}^{0\nu}$ are assumed. Experimental parameters (exposure, energy resolution, efficiency factors) are obtained from the original references or, when not available, extrapolated from the values used in GERDA. The best fit yields $N^{0\nu} = 0$ and a limit of

$$T_{1/2}^{0\nu} > 3.0 \times 10^{25} \text{ yr (90\% C.L.)}. \quad (4)$$

The Bayes factor is $P(H_1)/P(H_0) = 2 \times 10^{-4}$; the claim is hence strongly disfavored.

Whereas only ^{76}Ge experiments can test the claimed signal in a model-independent way, NME calculations can be used to compare the present ^{76}Ge result to the recent limits on the ^{136}Xe half-life from KamLAND-Zen [14] and EXO-200 [15]. Figure 2 shows the experimental results, the claimed signal [labeled “claim (2004)”], and the correlations for different predictions, assuming that the exchange of light Majorana neutrinos is the leading mechanism. Within this assumption, the present result can be also combined with the ^{136}Xe experiments to scrutinize Ref. [11]. The most conservative exclusion is obtained by taking the smallest ratio $M_{0\nu}(^{136}\text{Xe})/M_{0\nu}(^{76}\text{Ge}) \approx 0.4$ [27,28] of the calculations listed in Ref. [29]. This leads

to an expected signal count of 23.6 ± 5.6 (3.6 ± 0.9) for KamLAND-Zen (EXO-200). The comparison with the corresponding background-only models [30] yields a Bayes factor $P(H_1)/P(H_0)$ of 0.40 for KamLAND-Zen and 0.23 for EXO-200. Including the GERDA result, the Bayes factor becomes 0.0022. Also in this case the claim is strongly excluded; for a larger ratio of NMEs the exclusion becomes even stronger. Note, however, that other theoretical approximations might lead to even smaller ratios and thus weaker exclusions.

The range for the upper limit on the effective electron neutrino mass $m_{\beta\beta}$ is 0.2–0.4 eV. This limit is obtained by using the combined ^{76}Ge limit of Eq. (4), the recently reevaluated phase space factors of Ref. [32], and the NME calculations mentioned above [27,28,33–37]. Scaling due to different parameters g_A and r_A for NME is obeyed as discussed in Ref. [38].

In conclusion, due to the unprecedented low background counting rate and the good energy resolution intrinsic to HPGe detectors, GERDA establishes after only a 21.6 kg yr exposure the most stringent $0\nu\beta\beta$ half-life limit for ^{76}Ge . The long-standing claim for a $0\nu\beta\beta$ signal in ^{76}Ge is strongly disfavored, which calls for a further exploration of the degenerate Majorana neutrino mass scale. This will be pursued by GERDA phase II aiming for a sensitivity increased by a factor of about 10.

The GERDA experiment is supported financially by the German Federal Ministry for Education and Research (BMBF), the German Research Foundation (DFG) via the Excellence Cluster Universe, the Italian Istituto Nazionale di Fisica Nucleare (INFN), the Max Planck Society (MPG), the Polish National Science Centre (NCN), the Foundation for Polish Science (MPD programme), the Russian Foundation for Basic Research (RFBR), and the Swiss National Science Foundation (SNF). The institutions acknowledge also internal financial support. The GERDA Collaboration thanks the directors and the staff of LNGS for their continuous strong support of the GERDA experiment.

*Present address: CEGEP St-Hyacinthe, Québec, Canada.

†Present address: INFN LNGS, Assergi, Italy.

‡Also at Università di Firenze, Italy.

§Also at Moscow Institute of Physics and Technology, Russia.

||Also at International University for Nature, Society and Man, Dubna, Russia.

¶Present address: Shanghai Jiaotong University, Shanghai, China.

**Present address: University North Carolina, Chapel Hill, NC, USA.

††Also at Dipartimento di Science Fisica e Chimiche, University of L’Aquila, L’Aquila, Italy.

‡‡gerda-eb@mpi-hd.mpg.de

- [1] A. S. Barabash, *Phys. Rev. C* **81**, 035501 (2010).
- [2] V. I. Tretyak and Y. G. Zdesenko, *At. Data Nucl. Data Tables* **80**, 83 (2002).
- [3] S. M. Bilenki and C. Giunti, *Mod. Phys. Lett. A* **27**, 1230015 (2012).
- [4] J. D. Vergados, H. Ejiri, and F. Simkovic, *Rep. Prog. Phys.* **75**, 106301 (2012).
- [5] W. Rodejohann, *J. Phys. G* **39**, 124008 (2012).
- [6] J. J. Gómez Cadenas, J. Martin-Albo, M. Mezzetto, F. Monrabal, and M. Sorel, *Riv. Nuovo Cimento Soc. Ital. Fis.* **35**, 29 (2012).
- [7] B. J. Mount, M. Redshaw, and E. G. Myers, *Phys. Rev. C* **81**, 032501 (2010).
- [8] H. V. Klapdor-Kleingrothaus *et al.* (Heidelberg-Moscow Collaboration), *Eur. Phys. J. A* **12**, 147 (2001).
- [9] C. E. Aalseth *et al.* (IGEX Collaboration), *Phys. Rev. D* **65**, 092007 (2002).
- [10] C. E. Aalseth *et al.* (IGEX Collaboration), *Phys. Rev. D* **70**, 078302 (2004).
- [11] H. V. Klapdor-Kleingrothaus, I. V. Krivosheina, A. Dietz, and O. Chkvorets, *Phys. Lett. B* **586**, 198 (2004).
- [12] H. V. Klapdor-Kleingrothaus and I. Krivosheina, *Mod. Phys. Lett. A* **21**, 1547 (2006).
- [13] B. Schwingenheuer, *Ann. Phys. (Berlin)* **525**, 269 (2013).
- [14] A. Gando *et al.*, *Phys. Rev. Lett.* **110**, 062502 (2013).
- [15] M. Auger *et al.*, *Phys. Rev. Lett.* **109**, 032505 (2012).
- [16] K.-H. Ackermann *et al.* (GERDA Collaboration), *Eur. Phys. J. C* **73**, 2330 (2013).
- [17] Canberra Semiconductor NV, Lammerdries 25, B-2439 Olen, Belgium.
- [18] M. Agostini *et al.* (GERDA Collaboration), [arXiv:1306.5084](https://arxiv.org/abs/1306.5084).
- [19] M. Agostini, L. Pandola, P. Zavarise, and O. Volynets, *JINST* **6**, P08013 (2011).
- [20] M. Agostini, L. Pandola, and P. Zavarise, *J. Phys. Conf. Ser.* **368**, 012047 (2012).
- [21] D. Budjáš, M. Barnabé Heider, O. Chkvorets, N. Khanbekov, and S. Schönert, *JINST* **4**, P10007 (2009).
- [22] M. Agostini, C. A. Ur, D. Budjáš, E. Bellotti, R. Brugnera, C. M. Cattadori, A. di Vacri, A. Garfagnini, L. Pandola, and S. Schönert, *JINST* **6**, P03005 (2011).
- [23] M. Agostini *et al.* (GERDA Collaboration), [arXiv:1307.2610](https://arxiv.org/abs/1307.2610).
- [24] A. Caldwell and K. Kröninger, *Phys. Rev. D* **74**, 092003 (2006).
- [25] A. Caldwell, D. Kollar, and K. Kröninger, *Comput. Phys. Commun.* **180**, 2197 (2009).
- [26] Alternatively, the expected signal counts can be evaluated by rescaling the observed number of $0\nu\beta\beta$ decays of (28.75 ± 6.86) from Ref. [11] for the active exposure ($f_{av}\mathcal{E}$). All efficiency factors of Eq. (2) approximately cancel with the exception of ε_{PSD} . The expected number of events after the PSD selection is 6.8 (6.5 in $Q_{\beta\beta} \pm 2\sigma_E$). The difference to the above estimate of 5.9 counts is due to ε_{FEP} , which has been taken to be 100% in Ref. [11].
- [27] F. Simkovic, V. Rodin, A. Faessler, and P. Vogel, *Phys. Rev. C* **87**, 045501 (2013).
- [28] M. T. Mustonen and J. Engel, [arXiv:1301.6997](https://arxiv.org/abs/1301.6997).
- [29] P. S. Bhupal Dev, S. Goswami, M. Mitra, and W. Rodejohann, [arXiv:1305.0056](https://arxiv.org/abs/1305.0056).
- [30] The sensitivity of KamLAND-Zen corresponds to an equivalent background of 460 ± 21.5 counts. The equivalent observed counts are -1.17σ lower, i.e., about 435 events [31]. EXO-200 expects 7.5 ± 0.7 counts in the interval $Q_{\beta\beta} \pm 2\sigma_E$ and observes 5 events.
- [31] J. Bergström, *J. High Energy Phys.* **02** (2013) 093.
- [32] J. Kotila and F. Iachello, *Phys. Rev. C* **85**, 034316 (2012).
- [33] T. R. Rodriguez and G. Martinez-Pinedo, *Phys. Rev. Lett.* **105**, 252503 (2010).
- [34] J. Menendez, A. Poves, E. Caurier, and F. Nowacki, *Nucl. Phys. A* **818**, 139 (2009).
- [35] J. Barea, J. Kotila, and F. Iachello, *Phys. Rev. C* **87**, 014315 (2013).
- [36] J. Suhonen and O. Civitarese, *Nucl. Phys. A* **847**, 207 (2010).
- [37] A. Meroni, S. T. Petcov, and F. Simkovic, *J. High Energy Phys.* **02** (2013) 25.
- [38] A. Smolnikov and P. Grabmayr, *Phys. Rev. C* **81**, 028502 (2010).